HHS Public Access

Author manuscript

Nature. Author manuscript; available in PMC 2012 December 28.

Published in final edited form as:

Nature. 2012 June 28; 486(7404): 490–495. doi:10.1038/nature11163.

mTORC1 in the Paneth cell niche couples intestinal stem cell function to calorie intake

Ömer H. Yilmaz[1,2,#], **Pekka Katajisto**[2,#], **Dudley W. Lamming**[2], **Yetis Gültekin**[1,2], **Khristian E. Bauer-Rowe**[2], **Shomit Sengupta**[2], **Kivanc Birsoy**[2], **Abdulmetin Dursun**[1], **V. Onur Yilmaz**[2], **Martin Selig**[1], **G. Petur Nielson**[1], **Mari Mino-Kenudson**[1], **Lawrence Zukerberg**[1], **Atul Bhan**[1], **Vikram Deshpande**[1], and **David M. Sabatini**[2]

[1]Department of Pathology, Massachusetts General Hospital and Harvard Medical School, Boston, MA 02114 USA

[2]Whitehead Institute for Biomedical Research, Boston, MA 02142 USA; Department of Biology, MIT, Cambridge, MA 02139; Howard Hughes Medical Institute, MIT, Cambridge, MA 02139; Broad Institute of Harvard and MIT, Seven Cambridge Center, Cambridge, MA 02142; The David H. Koch Institute for Integrative Cancer Research at MIT, Cambridge, MA 02139

SUMMARY

How adult tissue stem and niche cells respond to the nutritional state of an organism is not well understood. Here, we find that Paneth cells, a key constituent of the mammalian intestinal stem cell (ISC) niche, augment stem cell function in response to calorie restriction (CR). CR acts by reducing mTOR complex 1 (mTORC1) signaling in Paneth cells, and the ISC-enhancing effects of CR can be mimicked by rapamycin. Calorie intake regulates mTORC1 in Paneth cells, but not ISCs, and forced mTORC1 activation in Paneth cells during CR abolishes their effects on ISCs. Finally, increased expression in Paneth cells of *bone stromal antigen 1* (*Bst-1*), an ectoenzyme that produces the paracrine factor cyclic ADP ribose (cADPR), mediates the effects of CR and rapamycin on ISC function. Our findings establish that mTORC1 non-cell autonomously regulates stem cell self-renewal, and highlight a significant role of the mammalian intestinal niche in coupling stem cell function to organismal physiology.

Mammalian tissue-specific stem cells maintain tissue homeostasis by undergoing either self-renewing or differentiation divisions that generate more stem cells or restricted progenitors, respectively[1]. Stem cells often require cues from their microenvironment or “niche” to regulate their fates. Caloric restriction (CR), an intervention in which caloric intake is reduced while maintaining adequate nutrition, promotes longevity in diverse organisms, possibly by preserving stem and progenitor cell function[2,3]. In mice, CR promotes the

Address correspondence to sabatini@wi.mit.edu.
[#]These authors contributed equally to this work.

Author Contributions ÖHY and PK designed and performed all experiments and data analyses with input from D.M.S. S.S. generated the Rheb2 transgenic mice. DWL, KB, VD, AB, MM, and LZ participated in design and interpretation of experiments. YG, OY, AD, KBR performed and interpreted all of the immunohistochemistry and in situ hybridization under the guidance of ÖHY. MS and PN performed electron microscopy and helped with its interpretation. ÖHY wrote the paper with help from PK and DMS.

generation of new neurons from neural progenitors and prevents the decline of hematopoietic stem cell numbers and function in certain strains of mice with age[2,4–7]. These findings raise the question of how CR mediates these effects on stem cells, and whether the mammalian stem cell niche is involved.

We have interrogated this question in the rapidly renewing mammalian small intestine. The intestine is organized into crypts that contain the stem cells and the rapidly dividing transient amplifying cells (TA-cells), and villi composed primarily of post-mitotic absorptive enterocytes. In response to fasting and refeeding the intestine undergoes structural alterations such as changes in villi length, crypt depth, and cell turnover, suggesting that organismal physiology may modify intestinal progenitor function[8,9]. Recent studies have begun to define the identity of intestinal stem cells as well as their interaction with their Paneth cell niche[10–15]. Although no single marker identifies the entire ISC pool, Lgr5 is expressed by a majority of ISCs throughout the intestinal tract[13,15]. Lgr5+ ISCs (aka crypt base columnar cells or CBCs) can self-renew and differentiate for the life of the organism, and they reside at the base of crypts sandwiched between Paneth cells[13,16]. Loss of Paneth cells *in vivo* leads to reduced numbers of Lgr5+ ISCs, while the addition of Paneth cells to *in vitro* cultures dramatically increases the potential of Lgr5+ ISCs to form multipotent, self-renewing organoid bodies reminiscent of “mini-intestines”[14]. Thus, Paneth cells constitute a critical component of the stem cell niche both *in vivo* and *in vitro*[13,14].

CR increases stem and niche cell numbers

To assess the effects of CR on intestinal homeostasis, we calorically restricted mice for 4 to 28 weeks, which is sufficient to observe many of the metabolic phenotypes of CR[17–19]. Consistent with prior reports, CR mice had a 19.7± 5.8% loss in body mass compared to *ad libitum* (AL) fed counterparts (Supplementary Fig. 1a)[20]. In CR mice the small intestine was morphologically normal (Supplementary Fig. 1f), with no change in crypt density (Supplementary Fig. 1d), intestinal length (Supplementary Fig. 1c), or apoptotic cell frequency (Supplementary Fig. 3). However, it did have reduced mass (1.8±0.4 vs 1.4±0.2g, Supplementary Fig. 1b) with villi that were 15% shorter and possessed fewer enterocytes (Supplementary Fig. 1e, f). CR did not affect the frequency of chromogranin A+ enteroendocrine cells, but mildly reduced that of alcian blue+ secretory goblet cells (Supplementary Fig 2a, b). To address how CR influenced the frequency of ISCs, we performed *in situ hybridization* for Olfactomedin-4 (Olfm4), a recently described marker that is co-expressed by Lgr5+ ISCs[21]. CR led to a 35% increase in Olfm4+ primitive intestinal progenitors compared to those in AL mice (Fig. 1a, Supplementary Fig. 6a). Interestingly, CR also caused a commensurate increase in Cryptdin4+ Paneth cells (Fig. 1a), which we confirmed by morphological examination of one-micron tissue sections (Supplementary Fig. 4a) and by electron microscopy (Supplementary Fig. 4b). These findings lead to two intriguing conclusions: First, CR promotes the preservation and self-renewal of ISCs (increased Olfm4+ ISCs) at the expense of differentiation (shorter villi with fewer mature enterocytes). Second, ISCs and their Paneth cells increase in tandem, raising the possibility that the Paneth cell niche may coordinate ISC adaptation to CR.

The fact that CR augmented ISC numbers while reducing the total number of differentiated enterocytes suggested that CR enhances the proliferation of ISCs while reducing the proliferation of more differentiated progenitors (TA-cells). To test this possibility, we assessed incorporation of BrdU into ISCs and TA-cells. After a 4 hour pulse of BrdU, CR-crypts had nearly 2-fold as many BrdU+ ISCs compared to AL-crypts (4.3±0.3 vs 2.4±0.2, Fig. 1b; Supplementary Fig. 1g, h). However, CR decreased the number of BrdU+ cells in the larger pool of TA-cells (11.0±0.9 vs 9.4±0.5; Fig. 1b), suggesting that output and migration into the villi from this compartment may also be reduced. Indeed, CR mice 24 hours after a single dose of BrdU had fewer absolute numbers of BrdU labeled cells in the villi compared to AL controls (14.5±1.5 vs 19.0±1.7, Supplementary Fig. 1i, j). However, there was no significant difference in the percentage of BrdU+ villous enterocytes, indicating that in CR mice TA-cells generate fewer progeny for shorter, less cellular villi (Supplementary Fig. 1k). These data demonstrate that CR alters the coupling between stem cell and TA-cell proliferation *in vivo*.

CR promotes intestinal regeneration

Because CR increased the frequency and proliferation of ISCs we asked whether it also promotes the regeneration of the small intestinal epithelium. We tested the potential of isolated crypts, independent of intestinal stem cell markers, to form clonal, multipotent organoid bodies that posses all intestinal cell types *in vitro*[22] (Supplementary Fig. 5). Crypts from CR mice were nearly 2-fold more likely to form organoid bodies than those from AL controls (Fig. 1c). These data suggest that CR leads to an increase in stem cell activity per crypt, as only stem cells are capable of self-renewing and differentiating into the various cell types that are required for organoid body formation and maintenance.

To ask whether CR also augments crypt regeneration *in vivo*, we used the clonogenic microcolony assay for testing ISC activity[23]. In AL and CR mice exposed to lethal doses of radiation and examined 72 hours later, CR significantly increased the number of surviving and regenerating crypts and Ki67+ intestinal progenitors per unit length of intestine (Fig. 1d, e). These data are consistent with our *in vivo* and *in vitro* data showing that CR increases the numbers and regenerative capacity of ISCs.

CR enhances ISC function via the niche

To understand how CR affects the frequency and function of ISCs and their Paneth cell niche, we performed CR experiments on *Lgr5-EGFP-IRES-CreERT2* knock-in mice, which allow isolation by flow cytometry of Lgr5-EGFP^{hi} ISCs and their daughter, more differentiated EGFP^{low} cells[16]. Compared to AL controls, CR increased the frequency of Lgr5-EGFP^{hi} ISCs (5.6±2.1% vs 4.3±1.9%, Fig. 1f) and Paneth cells (9.8±3.3% vs 6.7±3.3%, Fig. 1f, Supplementary Fig. 8, 9) by 1.5-fold. The frequency of the much larger pool of EGFP^{low} differentiated progenitors, however, was lower in CR (8.1±3.0% vs 10.1±4.3% Fig. 1f). These data corroborate the phenotypic expansion of ISCs and Paneth cells detected with the Olfm4 and Cryptdin4 markers, respectively (Fig.1a, Supplementary Fig. 6a, b), and suggest that while CR expands the pool of ISCs it leads to a reduction of

more differentiated progenitors. Thus, CR has opposing effects on the numbers of stem cells and their immediate progeny, shifting the equilibrium towards stem cell self-renewal.

The enhanced regenerative activity of CR-crypts led us to ask whether ISCs respond to CR autonomously or non-autonomously through the Paneth cells. To test this, we combined ISCs and Paneth cells isolated from CR and AL mice and assayed their ability to form organoid bodies in culture (Fig. 1g). Consistent with prior studies[14,22], neither Lgr5-EGFP^{hi} ISCs nor Paneth cells established organoid bodies on their own, but, when cocultured, 15% of ISCs did generate organoid bodies (Fig. 1g,h). Interestingly, Paneth cells isolated from CR mice were significantly more likely than those from AL controls to promote organoid body formation when mixed with ISCs (Fig. 1h), and this augmentation persisted even after 7 months of CR (Supplementary Fig. 6). In contrast, CR had neither a direct effect on ISC function (as CR or AL ISCs behaved similarly), nor did it boost the potential of EGFP^{low} progenitors to form organoid bodies (Fig. 1h, k). Ruling out the possibility that the enhancement caused by CR-Paneth cells resulted from an increase in their ability to home and attach to ISCs in culture, ISC-Paneth cell doublets isolated from CR mice had a 3-fold increase compared to those from AL mice in their capacity to form organoid bodies (Fig. 1j). Not only did CR-Paneth cells promote primary organoid body formation, these organoids gave rise to more and larger secondary organoid bodies, even when individually subcloned (Fig. 1i, l). Thus, individual organoid bodies from CR-Paneth cells posses a greater ability to self-renew (Fig. 1l). The fact that Lgr5-EGFP^{hi} ISCs form more organoid bodies when cocultured with CR-Paneth cells indicates that most Lgr5-EGFP^{hi} cells harbor stem cell potential when exposed to the appropriate niche signals (Fig. 1h, k).

Calorie intake activates mTORC1 in the niche

Because the mTORC1 (mechanistic target of rapamycin complex 1) kinase is a major sensor of the organismal nutritional state, we asked whether CR mediates its effects on Paneth cells through it[24]. Consistent with this, overnight fasting decreased phosphorylation of S6 (P-S6), a marker of mTORC1 activity in the intestine (Fig. 2a). Interestingly, feeding or insulin activated mTORC1 in Paneth cells but not in ISCs in a rapamycin-sensitive fashion (Fig. 2a). To confirm that we were observing Paneth cells, we cytospun isolated Paneth cells (>95% lysozyme+; Fig. 2b) and found that P-S6 expression was indeed induced in the Paneth cells of fasted mice by insulin administration. Similarly in immunoblots from isolated CR-crypts, phosphorylation of S6 and S6K1, the latter being a direct substrate of mTORC1, were diminished (Fig. 2c). These data suggest that Paneth cells may modulate ISC function by sensing the organismal nutritional status through mTORC1.

Niche mTORC1 mediates the effects of CR

To address whether reduced mTORC1 signaling in Paneth cells enhances ISC function in response to CR, we generated mice in which the expression of *Rheb2* (an mTORC1 activator) can be induced by doxycycline from the ubiquitously expressed ColA1 promoter (*Rheb*-tg) (Fig. 3a, b). In mice fasted overnight, induction of *Rheb2* was sufficient to reactivate mTORC1 signaling in Paneth cells (Fig. 3c, d). Interestingly, *Rheb2* induction during CR blocked the increase in clonogenicity per crypt (Fig. 3e) normally caused by CR,

prevented isolated Paneth cells from enhancing organoid formation when cultured with ISCs (Fig. 3f), and abolished the increase in Olfm4+ ISC and Cryptdin4+ Paneth cell numbers observed in CR *in vivo* (Supplementary Fig. 7a, b). To confirm that persistent mTORC1 activity negates the increase in Paneth cell frequency observed in CR, *TSC1*—a negative regulator of mTORC1—was excised using *TSC1*$^{loxp/loxp}$; *Rosa26-CreERT2* mice. The excision of *TSC1* during CR (similar to Rheb2 induction) prevented the increase in Paneth cell frequency as assessed by flow cytometry (Supplementary Fig. 7c). Thus, persistent mTORC1 activity during CR is sufficient to prevent CR-Paneth cells from promoting ISC function (Fig. 3e, f; Supplementary Fig. 7a–c).

As constitutive activation of mTORC1 abrogated the effects of CR, we asked whether inhibition of mTORC1 with rapamycin mimics the effects of CR. Indeed, administration of rapamycin to mice increased the frequency of ISCs and Paneth cells by more than 1.5-fold (Fig. 3g, h), and crypts isolated from mice treated for just 1 week with rapamycin were as capable of forming organoid bodies as those from mice on CR (Fig. 3i). Furthermore, rapamycin increased the clonogenicity of crypts irrespective of whether they were isolated from adult intestines expressing or lacking *Rictor*, a necessary and specific component of mTORC2 (Fig. 3k)[25]. These data indicate that rapamycin mediates this enhancement in crypt clonogenicity by inhibiting mTORC1 and does so independently of mTORC2.

Like CR, rapamycin acts non-autonomously because when Paneth cells isolated from rapamycin-treated mice were mixed with ISCs from control or rapamycin-treated mice, they caused a prominent increase in the formation of primary and subcloned secondary organoid bodies (Fig. 3j, l, m). Moreover, rapamycin treatment and CR did not have additive effects on either the ability of crypts (Fig. 3i) or Paneth cells (Fig. 3j, l) to form organoid bodies, suggesting that CR mediates many of its effects by reducing mTORC1. These data, together with the finding that CR and rapamycin have non-additive effects (Fig. 3i, j), demonstrate that CR and rapamycin indirectly promote ISC function and do so by reducing mTORC1 signaling in Paneth cells.

CR boosts *Bst-1* levels in Paneth cells

Several observations suggest that CR and rapamycin induce a state in Paneth cells that is quite stable. For example, Paneth cells taken from CR- or rapamycin-treated mice maintain their augmented capacity to promote ISC self-renewal even when placed in nutrient rich media that should activate mTORC1 (Fig. 1h, 3l). Similarly, Paneth cells isolated from mice that had been on CR, but were returned to an AL diet for 3 days, also retain an enhanced capacity to promote ISC function in the organoid assay (Fig. 1m). To gain mechanistic insight into how CR mediates its effects in Paneth cells, we undertook gene expression profiling of Paneth cells isolated by flow cytometry from AL and CR mice (n= 3 and 4, respectively). CR significantly changed the expression of 401 genes ($p<0.01$), including 57 that encode cell surface or secreted proteins; however, there were no changes in pathways previously implicated in mediating the Paneth cell and ISC interaction, such as Wnt or Notch (Fig. 4a, b, Supplementary Table 1)[14].

Of the genes upregulated by CR, we focused on *bone stromal antigen 1* (*Bst-1*) because its expression□ in bone marrow stromal cells promotes the proliferation of hematopoietic progenitors[26]. Bst-1 is an ectoenzyme that converts NAD+ to cyclic ADP ribose (cADPR), a paracrine effector that enters □responder cells via nucleoside transporters to activate calcium signaling and promote proliferation. CR increased *Bst-1* mRNA and protein expression in Paneth cells and caused a shift in its SDS-PAGE mobility suggestive of protein processing (Fig. 4b–e). Interestingly, while the addition of cADPR to crypt culture boosted the organoid-forming potential of AL-crypts, it did not augment the ability of CR-crypts to form organoids (Fig. 4e). Lastly, we asked whether *Bst-1* was necessary to mediate the effects of CR in the organoid formation assay (Fig. 4f, g). Indeed, knockdown of *Bst-1* mRNA with 2 independent functional siRNAs abrogated the enhanced capacity of CR-crypts to form organoids, and the addition of exogenous cADPR was sufficient to rescue the loss of Bst-1. These data demonstrate that CR, in an mTORC1-regulated manner, induces *Bst-1* in Paneth cells, that *Bst-1* is necessary to mediate many of the effects of CR, and that cADPR substitutes for *Bst-1* in the organoid assay.

Discussion

Our data favor a model in which the mammalian intestinal stem cell niche couples organismal nutritional status to stem cell function. Reduced calorie intake leads to more ISC self-renewal (expansion of phenotypic ISCs *in vivo*), an accompanying increase in the ISC niche, and to an increase in ISC function and regeneration *in vivo* and *in vitro*. Although it is unclear why CR increases ISC numbers and function, one possibility is that in low calorie conditions it may be advantageous for ISCs to slightly shift the balance towards self-renewal while reducing the pool and proliferation of more differentiated TA-cells. Preserving or increasing the stem cell pool may better prepare the intestine for rapid regeneration once nutrients become available and so enable organisms to adapt to periods of prolonged famine interspersed with times of abundant food.

Non-cell autonomous mechanisms also orchestrate intestinal remodeling in the Drosophila mid-gut, highlighting the importance of the stem cell niche as a sensor of organismal physiology in diverse species[27]. Fasting in Drosophila diminishes ISC numbers while refeeding dramatically expands them. In contrast, we find that CR in the murine intestine preserves the numbers of ISCs, but reduces the numbers and output of TA cells. Flexible intestinal adaptation in the fly gut occurs by direct modulation of ISCs, the only cells capable of proliferation, while in the murine intestine such adaptation can be achieved by differentially regulating ISCs and the larger, more proliferative pool of TA cells. In both systems, however, ISCs respond to organismal demands in part by niche signals.

CR mediates many of its effects on ISCs by reducing mTORC1 signaling in the ISC niche, emphasizing the importance of non-cell autonomous mechanisms in intestinal adaptation and regeneration. Moreover, our data raise the intriguing possibility that the use mTORC1 inhibitors or Bst-1 mimetics, such as FDA-approved drugs like rapamycin or cADPR, respectively, may have a use in improving intestinal regeneration and function in patients. It remains to be determined whether persistent mTORC1 activity in the ISC niche accounts for

intestinal atrophy in intestinal diseases, and whether CR or rapamycin treatment can improve intestinal regeneration in these patients.

Methods Summary

The *Rheb2* transgenic mouse was produced as described[28] using the human *Rheb2 (hsRheb2)* coding sequence. Mice used in this study include Lgr5-EGFP-IRES-CreERT2, Rosa26-CreERT2, UbiquitinC-CreERT2 (all obtained from the Jackson Laboratory), *Rictor*^{loxp}, and *TSC*^{loxp}. All were maintained on a C57BL/6 background. CR was achieved by providing individual or paired mice a daily portion of a chow diet fortified with vitamins and minerals amounting to 60% of the daily food intake of their ad libitum counterparts[20]. All mice used in CR experiments were between the ages of 10 to 24 weeks and were sacrificed prior to their daily feeding. Intestinal crypts and ISCs were isolated and cultured as adapted from[14,22]. Unless otherwise indicated, data are presented as means ± s.d and two-tailed Student's t-tests were used to assess statistical significance (*P<0.05, **P<0.01, ***P<0.001).

Materials and Method

Mice and Calorie restriction

Mice were housed in the Unit for Laboratory Animal Medicine at the Whitehead Institute for Biomedical Research. *Lgr5-EGFP-IRES-CreERT2* mice (Strain name: B6.129P2-Lgr5tm1(cre/ERT2)Cle/J, Stock Number: 008875) were purchased from Jackson Laboratories. *UbiquitinC-CreERT2* mice were obtained from the Jackson Laboratory (Strain Name: B6;129S-Tg(UBC-cre/ERT2)1Ejb/J, Stock Number: 007001). *Rictor* floxed mice were generated as described in[29] and backcrossed to C57BL/6 for at least 6 generations. *TSC1*$^{loxp/loxp}$ mice were the generous gift of D. Kwiatkowski (Harvard Medical School) and backcrossed to C57BL/6 for at least 6 generations. *Rosa26-CreERT2* mice (Rosa26 or R26) were obtained from the Jackson Laboratory (Strain Name: B6.129-*Gt(ROSA)26Sor*$^{tm1(cre/ERT2)Tyj}$/J, Stock Number 008463). CR was achieved by providing individual or paired mice a daily portion of a chow diet fortified with vitamins and minerals amounting to 60% of the daily food intake of their ad libitum counterparts[20]. All adult mice used in CR experiments were between the ages of 10 to 24 weeks and were sacrificed prior to their daily feeding. *Rictor* or *TSC1* was excised by treatment with tamoxifen suspended in corn or sunflower seed oil (Spectrum) at a concentration of 10 mg/mL, and 200 μl per 25 g of body weight was injected intraperitoneally into mice once daily for 5–7 days. Control animals received an equal volume of the tamoxifen suspension, but did not express the CreERT2 fusion protein. Mice were allowed to recover for at least 7 days after the last tamoxifen injection prior to any experiments. *In vivo* fate mapping in *Lgr5-EGFP-IRES-CreERT2;Rosa26*^{loxpstoploxp}*-LacZ* compound mice was done with a single injection of tamoxifen given at 200 μl per 25 g. As described previously[30], rapamycin (LC Laboratories) was administered by intraperitoneal injection for 7 to 28 consecutive doses at 4 mg/kg. It was reconstituted in absolute ethanol at 10 mg/ml and diluted in 5% Tween-80 (Sigma) and 5% PEG-400 (Hampton Research) before injection. The final volume of all injections was 200 μl. Regular insulin (Lilly) was administered at 0.75 U/kg diluted in PBS 20 minutes prior to sacrificing fasted mice.

Generation of Rheb2 Transgenic mouse

The *Rheb2* transgenic mouse was produced as described before in[28]. Briefly, mouse embryonic stem cells (KH2) were obtained containing a neomycin resistance gene as well as a hygromycin resistance gene lacking a promoter and an ATG start codon at the *ColA1* locus. The presence of frt sites flanking the neomycin and hygromycin resistant genes allows site-specific integration of the transgene at the *ColA1* locus. These embryonic cells also contain an M2rtTA transactivator at the endogenous *Rosa26* promoter, which, in the presence of doxycycline, leads to the transactivation of TetO-promoter driven transgenes. The human *Rheb2* (*hsRheb2*) coding sequence was cloned into a vector downstream of a TetO promoter that also contained a PKG-ATG-frt element necessary for frt-site integration. This vector, along with another vector contained the FLPe recombinase, were then electroporated into the KH2 cells. As a result, the coding sequence for *hsRheb2* along with a PGK promoter and the ATG initiation codon necessary for the expression of the hygromycin resistance gene is integrated into the genomic DNA of the KH2 cells at the *ColA1* locus. Cells with properly integrated *hsRheb2* were then selected by hygromycin resistance and subsequently injected into blastocysts. Chimeric mice were then mated with C57BL/6J mice until germline transmission of the transgene was achieved.

PCR genotyping of the *hsRheb2* transgenic mouse was performed with the following primers: *Rheb*-tg_F: CCAATTTGTGGAAGGCGAGTT, *Rheb2*-TG_R: CCATGGCCTTCATGTAGCTT

Immunohistochemistry/fluorescence

Tissues were fixed in 10% formalin, paraffin embedded, and sectioned. Antigen retrieval was performed with Borg Decloaker RTU solution (Biocare Medical) in a pressurized Decloaking Chamber (Biocare Medical) for 3 minutes. Antibodies: rat anti-BrdU (1:2000; Abcam 6326), rabbit phospho-S6 Ser235/236 (1:500, CST 4858), rabbit cleaved caspase 3 (1:500; CST 9664), rabbit chromogranin A (1:3000, Abcam 15160), rabbit Lysozyme (1:2000; Thermo), rabbit Bst-1 (1:1000, Abcam 74301) and mouse Bst-1 (1:100 to 500, BD Pharmingen). For mouse Bst-1, the M.O.M (mouse on mouse) kit was used according to the manufacturer's instructions (Vector labs PK-2200). Biotin conjugated secondary donkey anti-rabbit or rat antibodies were used from Jackson ImmunoResearch. The Vectastain Elite ABC immunoperoxidase detection kit (Vector Labs PK-6101) followed by Dako Liquid DAB+ Substrate (Dako) was used for visualization. For immunofluorescence Alexa Fluor 568 secondary antibodies (Invitrogen) were used. All antibody incubations were performed with Common Antibody Diluent (Biogenex)

In situ hybridization

The in situ probes used in this study correspond to expressed sequence tags or fully sequenced cDNAs obtained from Open Biosystems. The accession numbers (IMAGE mouse cDNA clone in parenthesis) for these probes are as follow: mouse *OLFM4* BC141127 (9055739), mouse *cryptdin4* BC134360 (40134597). To ensure the specificity of the probes, we generated both sense and antisense probes by in vitro transcription using DIG RNA labelling mix (Roche) according to the manufacturer's instructions and to previously published detailed methods[21,31].

Radiation and clonogenic microcolony assay

AL and CR adult mice were exposed to 15 Gy of ionizing irradiation from a 137-Cesium source (GammaCell) and sacrificed after 72 hours. The number of surviving crypts per length of the intestine was enumerated from H&E-stained sections.

Immunoblotting

Antibodies: rabbit anti phospho-T389 S6K1, phospho-S240/244 S6, S6K1, and S6 from CST; rabbit Bst-1 (ab74301) from Abcam; mouse anti □-actin (clone AC-15) from Sigma. Crypts or tissue were rinsed once with ice-cold PBS and lysed in ice-cold lysis buffer (50 mM HEPES [pH 7.4], 40 mM NaCl, 2 mM EDTA, 1.5 mM sodium orthovanadate, 50 mM NaF, 10 mM pyrophosphate, 10 mM glycerophosphate, and 1% Triton X-100, and one tablet of EDTA-free protease inhibitors [Roche] per 25 ml). The soluble fractions of cell lysates were isolated by centrifugation at 13,000 rpm for 10 min. Proteins extracts were denatured by the addition of sample buffer, boiled for 5 min, resolved by SDS-PAGE, and analyzed by immunoblotting.

Flow cytometry and isolation of ISCs and Paneth cells

Small intestines were removed and the fat/mesentery was dissected away. The intestinal lumen was washed with ice cold PBS (Mg-/Ca-) using a 18G feeding needle (Roboz FN-7905) until the intestines appeared white/pink. They were then opened longitudinally. The mucous was removed by gently rubbing the intestine between fingers in cold PBS. The intestines were cut into 3 to 5 mm fragments and placed into 50 ml conical tubes that were fill with ice cold 30 ml of PBS (Mg-/Ca-)/EDTA (10 mM). The samples were incubated and shook intermittently on ice for 30 minutes continuously discarding and replacing (at least 3 times) the supernatant. The fragments were then continually resuspended with ice cold 30ml PBS (Mg-/Ca-)/EDTA (10 mM) and intermittently shook on ice for 10 minutes, discarding the supernatant again for 3 times. The fragments were resuspended again with ice cold 30 ml PBS (Mg-/Ca-)/EDTA (10 mM) and incubated and intermittently shook while waiting on ice for 20 to 40 minutes. The samples were then triturated with a 10 ml pipette 1 to 2 times, and the contents were filtered twice through a 70-μm mesh (BD Falcon) into a 50 ml conical tube to remove villous material and tissue fragments. At this point the suspension was mainly composed of crypts. Crypts were removed from this step for crypt culture experiments and embeded in matrigel with crypt culture media. For ISC isolation, the crypt suspensions were centrifuged for 5 minutes at 250 g (4C or room temperature). The pellets were gently resuspended in 1.0 ml of undiluted TrypLE Express (Invitrogen) + 120 μl of DNase I (10U/μl, Roche) and transferred to 15 ml conical tubes. The samples were incubated in a 32° C water bath for 1.25 to 2 minutes, were not titurated, and were then placed on ice. 12 ml of cold SMEM was added to each sample and were gently triturated twice. The samples were then centrifuged for 5 minutes at 250 g. The pellets were resuspended and incubated for 15 minutes on ice in 0.5 to 1 ml SMEM that contained an antibody cocktail consisting of CD45-PE (eBioscience, 30-F11), CD31-PE (Biolegend, Mec13.3), Ter119-PE (Biolegend, Ter119), CD24-Pacific Blue (Biolegend, M1/69) and EPCAM-APC (eBioscience, G8.8). 12 ml of SMEM were added and the samples were centrifuged for 5 minutes at 250 g. The pellets were resuspended with 0.5–2 ml (depending

on the size of the pellet) of SMEM/ 7-AAD solution (1:500 dilution). The samples were filtered through a 40-μm mesh (BD Falcon) prior to cell sorting. ISCs were isolated as Lgr5-EGFP^{hi}Epcam^{+}CD24$^{low/-}$CD31^{-}Ter119^{-}CD45^{-}7-AAD^{-}, EGFP^{low} progenitors were isolated as EGFP^{low}Epcam^{+}CD24$^{low/-}$CD31^{-}Ter119^{-}CD45^{-}7-AAD^{-}, and Paneth cells were isolated as CD24^{hi}SideScatter^{hi}Lgr5-EGFP^{-}Epcam^{+}CD31^{-}Ter119-CD45^{-}7-AAD^{-} with a BD FACS Aria II SORP cell sorter into supplemented crypt culture medium. Dead cells were excluded from the analysis with the viability dye 7-AAD. When indicated, populations were cytospun (Thermo Cytospin 4) at 800 rpm for 2min, or allowed to settle at 37°C in fully humidified chambers containing 6% CO2 onto poly-L-lysine coated slides (Polysciences). The cells were subsequently fixed in 4% paraformaldehyde (pH=7.4, Electron Microscopy Sciences) prior to staining.

Crypt culture media

Isolated crypts were counted and embeded in matrigel (BD Bioscience 356231 growth factor reduced) that contains 1 μM Jagged (Ana-Spec) at 5–10 crypts/μl and cultured in a modified form of medium as described in[22]. Briefly, DMEM/F12 (Gibco) was supplemented by EGF 40 ng/ml (R&D), Noggin 200 ng/ml (Peprotech), R-spondin 500 ng/ml (R&D or Sino Biological), N-Acetyl-L-cysteine 1 μM (Sigma-Aldrich) and Y-27632 dihydrochloride monohydrate 20 ng/ml (Sigma-Aldrich). cADPR (Sigma), when indicated, was added to culture at 50 μM. 30–50 μl drops of matrigel with crypts were plated onto a flat bottom 48-well plate (Corning 3548) and allowed to solidify for 20 to 30 minutes in a 37° C incubator. 350 μl of crypt culture medium was then overlaid onto the matrigel, changed every other day, and maintained at 37°C in fully humidified chambers containing 6% CO2. Clonogenicity (colony-forming efficiency) was calculated by plating 50 to 400 crypts and assessing organoid formation 3 to 7 days after initiation of cultures.

Culture of isolated cells in supplemented crypt culture medium

Isolated ISCs or Paneth cells were centrifuged for 5 minutes at 250 g and then resuspended in the appropriate volume of crypt culture medium (500–1000cells/μl) supplemented with 1× N2 (Invitrogen), 1× B27 (Invitrogen), 100 ng/ml Wnt-3A (R&D), and with additional 500 ng/ml R-Spondin to yield 1 μg/ml final concentration. ISCs were then seeded into matrigel (BD Bioscience 356231 growth factor reduced) containing 1 μM Jagged (Ana-Spec) up to 5,000–10,000 cells/30–50 μl. 30 μl drops of 65% matrigel were plated onto a flat bottom 48-well plate (Corning 3548) and then Paneth cells were added at the same cell count to the top of the matrigel drop. Alternatively, ISCs and Paneth cells were mixed after sorting in a 1:1 ratio, centrifuged, and then seeded into matrigel. The matrigel drops with ISCs and Paneth cells were allowed to solidify for 20 to 30 minutes in a 37° C incubator. 350 μl of crypt culture medium was then overlayed onto the drops of matrigel and maintained at 37°C in fully humidified chambers containing 6% CO2. The crypt media was changed every second day. Organoid bodies were quantitated on days 3, 7, and 9 days of culture, unless otherwise specified. In subcloning experiments, either individual or cultures of organoids were manually disrupted as indicated in the text on day 7–9 by rigorous tituration and replated into fresh matrigel; these secondary organoid bodies were quantitated on day 18 after initiation of the primary cultures. When indicated, crypts were transfected with 100nM siRNAs targeting the *Bst-1* (Thermo Scientific, J-044021-11 and J-044021-12) using the X-

Tremegene siRNA transfection reagent, by incubating the crypts at +37°C for 30 min with transfection mixture in crypt medium before mounting to matrigel.

Microarray analysis and validation

Approximately 100,000 Paneth cells were harvested directly to the RLT buffer of the RNeasy plus extraction kit (Qiagen) by the flowcytometry isolation protocol. Total RNA extracts were subjected to microarray analysis by standard protocols of the Whitehead Institute Genome Technology Core (http://jura.wi.mit.edu/genomecorewiki/index.php/Main_Page) using GeneChip Mouse Gene 1.0 ST arrays (Affymetrix). Expression analysis was conducted with the help of Whitehead Institute Bioinformatics and Research Computing. Briefly, CEL-files were preprocessed with RMA using Bioconductor and the package oligo, and differential expression was assayed by moderated t-test, as implemented by limma. Expression changes were validated by qRT-PCR using oligos:

Bst-1 ACCCCATTCCTAGGGACAAG, GCCTCCAATCTGTCTTCCAG,

Wnt3a GGGAGAAATGCCACTGTGTT, TCTCCGCCCTCAAGTAAGAA,

Myc TCTCCACTCACCAGCACAAC, TCGTCTGCTTGAATGGACAG,

Gapdh TGTTCCTACCCCCAATGTGT, TGTGAGGGAGATGCTCAGTG

Electron Microscopy

Immediately after removal from the animal, 1.0 mm sections of mouse intestine were placed into Karnovsky's KII Solution (2.5% glutaraldehyde, 2.0% paraformaldehyde, 0.025% calcium chloride, in a 0.1 M sodium cacodylate buffer, pH 7.4), fixed overnight at 4° C, and stored in cold buffer. Subsequently, they were post-fixed in 2.0% osmium tetroxide, stained en bloc with uranyl acetate, dehydrated in graded ethanol solutions, infiltrated with propylene oxide/Epon mixtures, flat embedded in pure Epon, and polymerized over night at 60°C. One micron sections were cut, stained with toluidine blue, and examined by light microscopy. Representative areas were chosen for electron microscopic study and the Epon blocks were trimmed accordingly. Thin sections were cut with an LKB 8801 ultramicrotome and diamond knife, stained with Sato's lead, and examined in a FEI Morgagni transmission electron microscope. Images were captured with an AMT (Advanced Microscopy Techiques) 2K digital CCD camera.

Supplementary Material

Refer to Web version on PubMed Central for supplementary material.

Acknowledgements

This work was supported by the National Institutes of Health (CA103866 and CA129105 to D.M.S.), the Koch Institute (Initiator award to D.M.S.), Ellison Medical Foundation (D.M.S.), the Warshaw Institute from the Massachusetts General Hospital (Ö.H.Y.), and the Center for Inflammatory Diseases from the Massachusetts General Hospital (Ö.H.Y. and D.M.S.), and fellowship support from the NCI (T32CA09216 to the Department of Pathology at the MGH to Ö.H.Y.), the Academy of Finland and the Foundations' Post Doc Pool (P.K.), the NIH (1F32AG032833-01A1 to D.W.L.) and Jane Coffin Childs Medical Fund (K.B.). We thank Patti Wisniewski and Chad Araneo of the Whitehead flow cytometry core facility, the Whitehead Genome Technology Core and Bioinformatics and Research Computing, Sven Holder for histology and help with special stains, Kathleen Ottina

for lab management, and Amanda Hutchins for animal husbandry and genotyping. D.M.S. is an investigator of the Howard Hughes Medical Institute.

Microarray data have been deposited in the GEO database under accession number GSE37209.

References

1. Simons BD, Clevers H. Strategies for homeostatic stem cell self-renewal in adult tissues. Cell. 145:851–862. doi:S0092-8674(11)00594-0 [pii] 10.1016/j.cell.2011.05.033. [PubMed: 21663791]
2. Nakada D, Levi BP, Morrison SJ. Integrating physiological regulation with stem cell and tissue homeostasis. Neuron. 70:703–718. doi:S0896-6273(11)00392-8 [pii] 10.1016/j.neuron.2011.05.011. [PubMed: 21609826]
3. McCay CM, Maynard LA, Sperling G, Barnes LL. The Journal of Nutrition. Volume 18 July--December, 1939. Pages 1--13. Retarded growth, life span, ultimate body size and age changes in the albino rat after feeding diets restricted in calories. Nutr Rev. 1975; 33:241–243. [PubMed: 1095975]
4. Bondolfi L, Ermini F, Long JM, Ingram DK, Jucker M. Impact of age and caloric restriction on neurogenesis in the dentate gyrus of C57BL/6 mice. Neurobiol Aging. 2004; 25:333–340. doi: 10.1016/S0197-4580(03)00083-6 S0197458003000836 [pii]. [PubMed: 15123339]
5. Ertl RP, Chen J, Astle CM, Duffy TM, Harrison DE. Effects of dietary restriction on hematopoietic stem-cell aging are genetically regulated. Blood. 2008; 111:1709–1716. doi:blood-2007-01-069807 [pii] 10.1182/blood-2007-01-069807. [PubMed: 17947508]
6. Chen J, Astle CM, Harrison DE. Hematopoietic senescence is postponed and hematopoietic stem cell function is enhanced by dietary restriction. Exp Hematol. 2003; 31:1097–1103. [PubMed: 14585375]
7. Yilmaz OH, Kiel MJ, Morrison SJ. SLAM family markers are conserved among hematopoietic stem cells from old and reconstituted mice and markedly increase their purity. Blood. 2006; 107:924–930. [PubMed: 16219798]
8. Dunel-Erb S, et al. Restoration of the jejunal mucosa in rats refed after prolonged fasting. Comp Biochem Physiol A Mol Integr Physiol. 2001; 129:933–947. [PubMed: 11440878]
9. Altmann GG. Influence of starvation and refeeding on mucosal size and epithelial renewal in the rat small intestine. The American journal of anatomy. 1972; 133:391–400. doi:10.1002/aja.1001330403. [PubMed: 5016502]
10. Zhu L, et al. Prominin 1 marks intestinal stem cells that are susceptible to neoplastic transformation. Nature. 2009; 457:603–607. doi:nature07589 [pii] 10.1038/nature07589. [PubMed: 19092805]
11. Sangiorgi E, Capecchi MR. Bmi1 is expressed in vivo in intestinal stem cells. Nat Genet. 2008; 40:915–920. doi:ng.165 [pii] 10.1038/ng.165. [PubMed: 18536716]
12. Breault DT, et al. Generation of mTert-GFP mice as a model to identify and study tissue progenitor cells. Proc Natl Acad Sci U S A. 2008; 105:10420–10425. doi:0804800105 [pii] 10.1073/pnas.0804800105. [PubMed: 18650388]
13. Barker N, et al. Identification of stem cells in small intestine and colon by marker gene Lgr5. Nature. 2007; 449:1003–1007. doi:nature06196 [pii] 10.1038/nature06196. [PubMed: 17934449]
14. Sato T, et al. Paneth cells constitute the niche for Lgr5 stem cells in intestinal crypts. Nature. 2011; 469:415–418. doi:10.1038/nature09637. [PubMed: 21113151]
15. Takeda N, et al. Interconversion between intestinal stem cell populations in distinct niches. Science. 2011; 334:1420–1424. doi:10.1126/science.1213214. [PubMed: 22075725]
16. Snippert HJ, et al. Intestinal crypt homeostasis results from neutral competition between symmetrically dividing Lgr5 stem cells. Cell. 143:134–144. doi:S0092-8674(10)01064-0 [pii] 10.1016/j.cell.2010.09.016. [PubMed: 20887898]
17. Hempenstall S, Picchio L, Mitchell SE, Speakman JR, Selman C. The impact of acute caloric restriction on the metabolic phenotype in male C57BL/6 and DBA/2 mice. Mech Ageing Dev. 2010; 131:111–118. doi:S0047-6374(10)00003-5 [pii] 10.1016/j.mad.2009.12.008. [PubMed: 20064544]

18. Cohen DE, Supinski AM, Bonkowski MS, Donmez G, Guarente LP. Neuronal SIRT1 regulates endocrine and behavioral responses to calorie restriction. Genes Dev. 2009; 23:2812–2817. doi: 23/24/2812 [pii] 10.1101/gad.1839209. [PubMed: 20008932]
19. Spindler SR. Rapid and reversible induction of the longevity, anticancer and genomic effects of caloric restriction. Mechanisms of Ageing and Development. 2005; 126:960–966. doi:10.1016/j.mad.2005.03.016. [PubMed: 15927235]
20. Kalaany NY, Sabatini DM. Tumours with PI3K activation are resistant to dietary restriction. Nature. 2009; 458:725–731. doi:nature07782 [pii] 10.1038/nature07782. [PubMed: 19279572]
21. van der Flier LG, et al. Transcription factor achaete scute-like 2 controls intestinal stem cell fate. Cell. 2009; 136:903–912. doi:S0092-8674(09)00079-8 [pii] 10.1016/j.cell.2009.01.031. [PubMed: 19269367]
22. Sato T, et al. Single Lgr5 stem cells build crypt-villus structures in vitro without a mesenchymal niche. Nature. 2009 doi:nature07935 [pii] 10.1038/nature07935.
23. Marsh V, et al. Epithelial Pten is dispensable for intestinal homeostasis but suppresses adenoma development and progression after Apc mutation. Nat Genet. 2008; 40:1436–1444. doi:ng.256 [pii] 10.1038/ng.256. [PubMed: 19011632]
24. Sengupta S, Peterson TR, Laplante M, Oh S, Sabatini DM. mTORC1 controls fasting-induced ketogenesis and its modulation by ageing. Nature. 468:1100–1104. doi:nature09584 [pii] 10.1038/nature09584. [PubMed: 21179166]
25. Sarbassov DD, et al. Prolonged rapamycin treatment inhibits mTORC2 assembly and Akt/PKB. Mol Cell. 2006; 22:159–168. doi:S1097-2765(06)00218-8 [pii] 10.1016/j.molcel.2006.03.029. [PubMed: 16603397]
26. Podesta M, et al. Concentrative uptake of cyclic ADP-ribose generated by BST-1 + stroma stimulates proliferation of human hematopoietic progenitors. The Journal of biological chemistry. 2005; 280:5343–5349. doi:10.1074/jbc.M408085200. [PubMed: 15574424]
27. O'Brien LE, Soliman SS, Li X, Bilder D. Altered modes of stem cell division drive adaptive intestinal growth. Cell. 2011; 147:603–614. doi:10.1016/j.cell.2011.08.048. [PubMed: 22036568]
28. Beard C, Hochedlinger K, Plath K, Wutz A, Jaenisch R. Efficient method to generate single-copy transgenic mice by site-specific integration in embryonic stem cells. Genesis. 2006; 44:23–28. doi: 10.1002/gene.20180. [PubMed: 16400644]
29. Guertin DA, et al. mTOR complex 2 is required for the development of prostate cancer induced by Pten loss in mice. Cancer Cell. 2009; 15:148–159. doi:S1535-6108(08)00436-4 [pii] 10.1016/j.ccr.2008.12.017. [PubMed: 19185849]
30. Yilmaz OH, et al. Pten dependence distinguishes haematopoietic stem cells from leukaemia-initiating cells. Nature. 2006; 441:475–482. [PubMed: 16598206]
31. Gregorieff A, Clevers H. In situ hybridization to identify gut stem cells. Curr Protoc Stem Cell Biol. Chapter 2 Unit 2F 1, doi:10.1002/9780470151808.sc02f01s12.

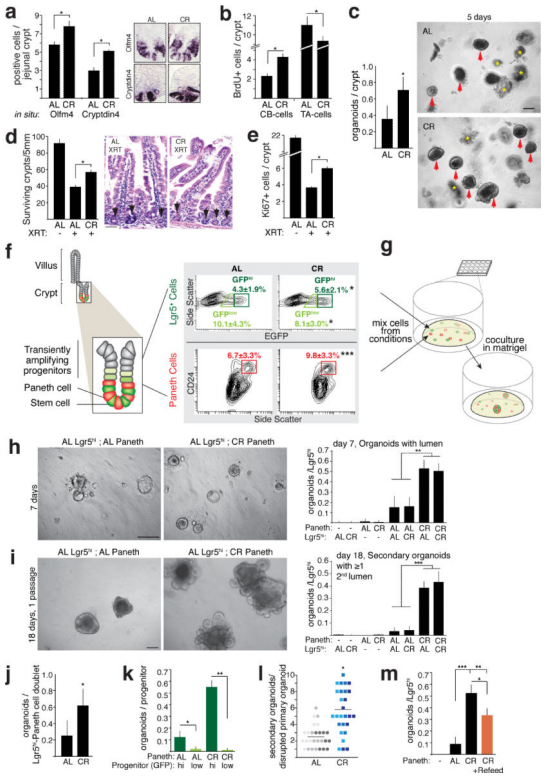

Figure 1. Calorie restriction augments the capacity of Paneth cells to boost ISC function

a. Olfm4+ ISCs and Cryptdin4+ Paneth cells were increased in CR mice (*in situ hybridization*, proximal jejunum, n=3). **b.** Crypt base columnar cells (CB-cells) showed a 2-fold increase in BrdU incorporation and TA-cells revealed a reduction after a 4-hour pulse in CR mice (n=3). **c.** CR-crypts were 2-fold more capable of forming organoids (n=8). Representative AL and CR-organoids are shown at 5 days (red arrowhead marks organoids and yellow asterisk indicates aborted crypts; scale bar = 50 μm). **d**–**e.** CR increased the number of surviving (**d**) and proliferating (**e,** Ki67+) crypts after irradiation induced damage (n=3 for d and e). **f.** Schematic demonstrating dark green Lgr5^{hi} ISCs, red Paneth cells, and light green EGFP^{low} progenitors. CR increased ISCs (dark green) and Paneth cells (red) by 1.5-fold, and reduced EGFP^{low} (light green) progenitors by 20% (CR, n=27; AL, n=26). **g.** A schematic illustrating the mixing of ISCs with Paneth cells in matrigel. **h.** Organoid formation per Lgr5^{hi} ISCs cocultured with Paneth cells from CR mice was significantly increased (n=5). Representative image of primary organoids at day 7. **i.** Dissociated organoids derived from CR-Paneth cells gave rise to larger secondary organoids at day 18 (n=5). **j.** Sorted ISC-Paneth cell doublets plated at clonal density (50–100 doublets per 30 ul droplet of matrigel) demonstrated that CR-doublets had nearly 3-fold more organoid potential (n=3). **k**. EGFP^{low} progenitors harbored little organoid potential (n=4). **l.** Subcloning of individual CR-Paneth derived organoids gave rise to 3-fold more secondary organoids (27 organoids from 3 independent mice per condition were analyzed, shades of grey or blue denote separate mice). **m.** Paneth cells isolated from mice that had been on CR, but were returned to an AL diet for 3 days, also retained an augmented capacity to promote

organoid formation (n=3). (Unless other wise indicated, in all panels: values = mean; error bars = s.d.; scale bars= 50 μm; * indicates P<0.05; ** P<0.01; and *** P<0.001).

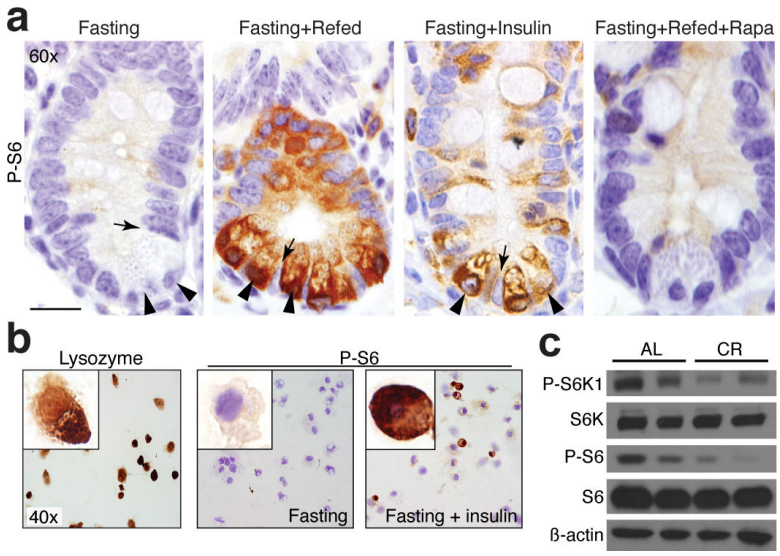

Figure 2. Nutritional regulation of mTORC1 in Paneth cells

a. Overnight fasted mice treated without or with rapamcyin were refed for 5 hours and intestinal sections immunostained for phospho-S6 (P-S6). Refeeding or administration of insulin activates mTORC1 in Paneth cells (arrow heads) but not ISCs (arrows, n=3–5, scale bar = 20 μm). **b.** Similar results were observed in cytospun preparations of sorted Paneth cells that were confirmed to be greater than 95% positive for the Paneth cell marker Lysozyme (n=3). P-S6 was reduced in sorted Paneth cells from fasted mice and was induced 20 minutes after injection with insulin. **c.** Immunoblots of isolated crypts from CR mice show reduced phosphorylation of known mTORC1 substrates phospho-S6K1 (P-S6K1) and P-S6.

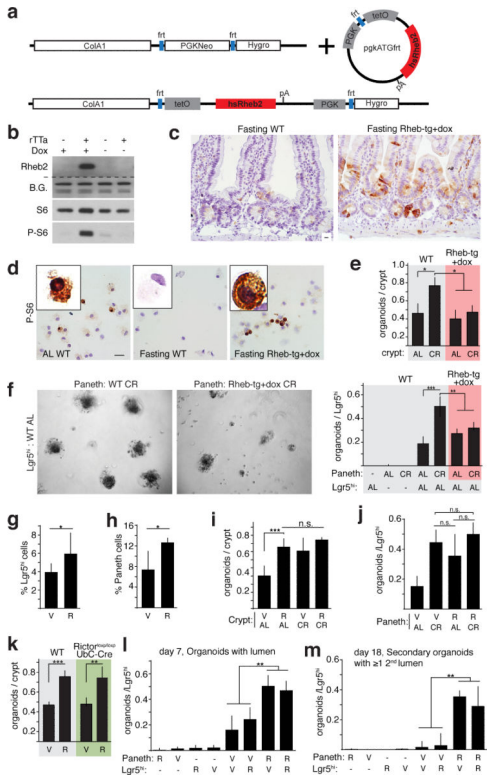

Figure 3. mTORC1 signaling in Paneth cells mediates the effects of calorie restriction on ISC function

a. Schematic of the Tet-ON human *Rheb2* transgene (*Rheb*-tg). **b.** Doxycycline (dox) induced Rheb2 protein and S6 phosphorylation in the liver (background band: B.G.). **c**–**d.** Fasted *Rheb*-tg mice demonstrated increased immunostaining of P-S6 in intestinal epithelium (c) and in isolated Paneth cells (d) upon dox injection. **e**–**f.** Induction of *Rheb2* from the start of CR abrogated the enhancement in organoid formation per crypt (n=3) (**e**) and per Lgr5^{hi} ISC cocultured with Paneth cells (n=5) (**f**). **g**–**h.** Rapamycin (R) (n=13) increased the frequency of Lgr5^{hi} ISCs (**g**) and Paneth cells (**h**) compared to vehicle (V) (n=14) as measured by flow cytometry. **i**–**j.** Organoid potential of intestinal crypts (n=3) (**i**) and AL Lgr5^{hi} ISCs with Paneth cells (n=5) (**j**) from R, CR, or CR+R treated mice. **k.** Rapamycin increased crypt organoid formation in Rictor deleted *Rictor$^{fl/fl}$UBC-CreERT2* mice (n=3) to a similar extent as in wild-type (WT) mice. **l.** Organoid formation of Lgr5^{hi} ISCs combined with Paneth cells from rapamycin treated mice was significantly increased in comparison to Paneth cells from vehicle treated mice (n=5). **m**. Dissociated primary organoids derived from R-Paneth cells gave rise to more secondary organoids (n=5). (Unless otherwise indicated, in all panels: values = mean; error bars = s.d.; scale bars= 20 μm; * indicates P<0.05; ** P<0.01; and *** P<0.001).

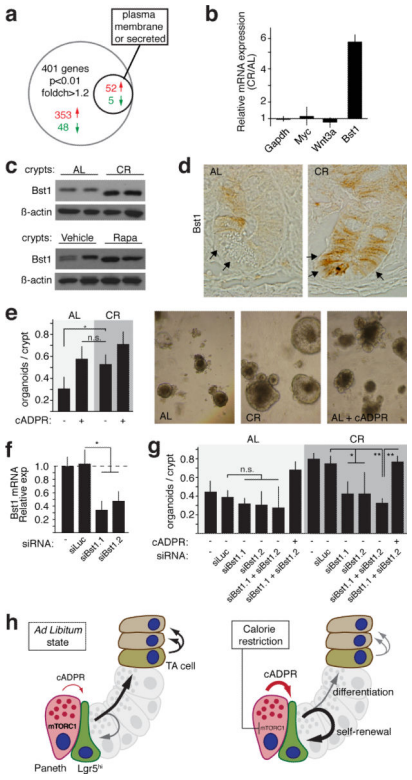

Figure 4. Calorie restriction enhances expression of *bone stromal antigen 1 (Bst-1)* in Paneth cells, whose product cyclic ADP ribose (cADPR) enhances ISC function

a. Transcriptional profiling of Paneth cells from CR and AL mice (n=4 and 3, respectively) identified significant expression changes in 401 genes, 57 of which encode plasma membrane associated or secreted proteins. **b.** Validation of the increased transcription of *Bst-1* by qRT-PCR (n=3). **c**–**d.** Increased Bst-1 protein in crypts from CR mice and rapamycin treated mice detected via immunoblotting (**c**) and in CR-Paneth cells by immunostaining (**d**). **e**. Exogenous cADPR increased the organoid potential of AL-crypts to an extent similar as those of CR-crypts (n=3). **f**–**g** Inhibition of *Bst-1* by siRNA-mediated knock-down (n=3) (**f**) abrogated the enhanced potential of CR-crypts to form organoids (n=3) (**g**). **i**. A model of intestinal adaptation to calorie restriction by non-cell autonomous regulation of ISC self-renewal. CR attenuates mTORC1 activity in the Paneth cells, resulting in increased expression of *Bst-1*, whose paracrine product cADPR promotes ISC self-renewal. * indicates P<0.05; ** P<0.01, *** P<0.001. Values = means and error bars = s.d.